

Phonons and rotons in commensurate p -H₂ and o -D₂ monolayers on graphite

W. B. J. M. Janssen, T. H. M. van den Berg, and A. van der Avoird

Institute of Theoretical Chemistry, University of Nijmegen, Toernooiveld, 6525 ED Nijmegen, The Netherlands

(Received 19 July 1990)

For the commensurate $(\sqrt{3} \times \sqrt{3})R30^\circ$ phase of p -H₂ and o -D₂ on graphite, we have calculated the phonon and roton band structures by the time-dependent Hartree method. A basis of three-dimensional harmonic-oscillator functions (up to $n=8$ inclusive) is used for the translational vibrations and a basis of spherical harmonics for the weakly hindered rotations. The anisotropic potential between the molecules in the adsorbed layer is taken from *ab initio* calculations. An anisotropic molecule-substrate potential is modeled semiempirically. Both potentials are explicitly expanded with respect to the molecular displacements, with the inclusion of high anharmonic terms, and with respect to their anisotropy. Moreover, the molecule-substrate potential is Fourier expanded to expose the effects of the surface corrugation. The structure of the in-plane phonon band agrees well with the data available from inelastic neutron scattering. For the peak that has been ascribed previously to the out-of-plane phonon band, we suggest an alternative assignment. For the rotons we have derived, both numerically and analytically, the dependence of the band structure on the (unknown) anisotropy of the molecule-substrate potential.

I. INTRODUCTION

A subject that has aroused interest recently is the structure and dynamics of H₂ and D₂ layers physisorbed on the basal plane of graphite. A variety of adsorbed phases and transitions between these phases have been identified by means of low-energy electron diffraction (LEED), neutron-diffraction, and specific-heat measurements.¹⁻⁹ For the commensurate $(\sqrt{3} \times \sqrt{3})R30^\circ$ phase, which occurs up to 1.08 monolayer coverage for H₂ and up to 1.05 monolayer coverage for D₂ at temperatures below 20 K, the dynamics also has been investigated by inelastic neutron scattering (INS).¹⁰⁻¹⁵ Although it was not possible to study single crystals and thus to measure directly the full two-dimensional phonon dispersion curves, an elegant experimental setup and interpretation allowed the determination of phonon frequencies for different points in the two-dimensional Brillouin zone.

The motions and stability of these H₂ and D₂ overlayers on graphite are determined by an interplay between the intermolecular interactions in the adsorbed layers and the interactions of the adsorbed molecules with the periodic substrate. The $(\sqrt{3} \times \sqrt{3})R30^\circ$ phase can be considered as a two-dimensional molecular crystal with a nearest-neighbor distance of 4.26 Å (which is substantially larger than the nearest-neighbor distances of 3.79 and 3.61 Å in bulk hydrogen and deuterium). Because of this large lattice spacing and the small masses of H₂ and D₂, the molecules exert large, and probably strongly anharmonic, zero-point motions. The quantum nature of these systems is most evident from the molecular rotations, however. One expects to find nearly free rotations of the molecules in the layers, characterized by quantum numbers j and m . Even values of j occur for p -H₂ and o -D₂, odd- j values for o -H₂ and p -D₂. Due to the large rotational energy splittings between different j states, the

molecular rotations are just weakly perturbed by the anisotropic environment and weakly coupled by anisotropic intermolecular interactions. So the ground state of p -H₂ and o -D₂ is orientationally disordered with nearly spherical ($j=0$) molecules and collective rotational excitations to a $j=2$ roton band. Also o -H₂ and p -D₂ are orientationally disordered, except at very low temperatures^{16,17} where the $j=1$ ground state is split into states with $m=0$ and ± 1 . Most experimental studies¹⁻¹⁵ concern these orientationally disordered phases of *para*-, *ortho*-, or mixed (normal) hydrogen and deuterium layers.

It will be obvious from these considerations that the standard (harmonic) lattice-dynamics method and the classical molecular-dynamics (MD) method which are usually applied to the ordered and disordered phases of molecular crystals and, more recently, also to adsorbed layers, cannot be applied here. Gotlieb and Bruch^{18,19} have calculated the vibrational ground state of H₂ and D₂ layers adsorbed on graphite by a variational quantum Monte Carlo method. Their vibrational wave function was a product of single-molecule functions for the center-of-mass vibrations, multiplied by a Jastrow function to account for the correlation between these vibrations. The molecules were assumed to be effectively spherical and, thus, to interact via an isotropic pair potential. The center-of-mass vibrations were restricted to be planar, i.e., parallel to the graphite surface. Novaco²⁰ has shown that it is essential to also include the displacements of the molecules perpendicular to the surface, even if one is primarily interested in their vibrations in the parallel directions. He has calculated the dispersion relations for the in-plane phonons in commensurate H₂ and D₂ layers on graphite by means of the self-consistent phonon (SCP) method and found the results to be in good agreement with the available INS data.¹⁰⁻¹⁵ In this calculation it was also assumed that the H₂ and D₂ mole-

cules are effectively spherical and interact via isotropic potentials. This assumption was verified by Novaco and Wroblewski²¹ who calculated the single-molecule rotational states in H₂, HD, and D₂ layers on graphite in the anisotropic field originating from the substrate. The anisotropic interactions between the adsorbed molecules were neglected, however.

In the present calculations for commensurate ($\sqrt{3} \times \sqrt{3}$)R 30° layers of H₂ and D₂ on the basal plane of graphite, we compute both the in-plane and the out-of-plane phonon states, as well as the collective rotational (roton) states and their coupling to the phonon states (which appears to be small indeed). We use the full anisotropic intermolecular potential for hydrogen from *ab initio* calculations.^{22,23} For the molecule-substrate interaction we construct an anisotropic model potential which generalizes the isotropic H₂-graphite potential obtained from selective adsorption measurements^{24,25} (in the same way as Novaco and Wroblewski did.²¹). Phonon, roton, and possibly mixed, states are calculated by means of the time-dependent Hartree (TDH) method. Basis functions at the first (mean-field) level of this calculation are the free rotor functions of H₂ or D₂ (spherical harmonics) and three-dimensional harmonic-oscillator functions for the center-of-mass vibrations of the molecules. This TDH method with the same *ab initio* H₂-H₂ potential has been applied previously to H₂ and D₂ solids.²⁶ It was found, even for the smaller nearest-neighbor separations that occur in these bulk solids, that the use of Jastrow functions for the correlation between the center-of-mass vibrations could be avoided if the full anharmonicity of the intermolecular potential was included and the harmonic-oscillator basis for these center-of-mass vibrations was sufficiently large, so that the wave functions at the mean-field level could adapt to this anharmonicity. Results are presented for commensurate *p*-H₂ and *o*-D₂ layers on graphite; in a forthcoming paper we will discuss results for *o*-H₂ and *p*-D₂ overlayers.

II. THEORY

A. The Hamiltonian

The center-of-mass positions of the molecules in the adsorbed layer are denoted by $\mathbf{r}_p = \mathbf{R}_p + \mathbf{u}_p$, where \mathbf{R}_p are the equilibrium positions and \mathbf{u}_p are the displacements of the molecules *p*. The orientations of the molecules are described by a set of polar angles ω_p . We assume that the motions of the molecules in the adsorbed layer are separable from the graphite lattice vibrations which have much higher frequencies and small amplitudes. We use a rigid graphite substrate so that the molecule-substrate potential V_p for a given molecule *p* depends only on the coordinates \mathbf{u}_p and ω_p of that molecule. The pair potential between the molecules within the adsorbed layer is denoted by $\Phi_{pp'}$. Many-body interactions, as well as substrate-mediated interactions between the adsorbed molecules are neglected. Then, the Hamiltonian for the adsorbed layer is given by

$$H = \sum_p T(\mathbf{u}_p) + \sum_p L(\omega_p) + \sum_p V_p(\mathbf{u}_p, \omega_p) + \frac{1}{2} \sum_p \sum_{p' \neq p} \Phi_{pp'}(\mathbf{u}_p, \omega_p, \mathbf{u}_{p'}, \omega_{p'}) . \quad (1)$$

It contains the kinetic-energy terms for the translational center-of-mass motions T and the rotational motions L of the molecules, the molecule-substrate potential, and the intermolecular potential.

In the mean-field formalism the translational and rotational Hamiltonians are given by

$$H_p^T(\mathbf{u}_p) = T(\mathbf{u}_p) + \langle V_p(\mathbf{u}_p, \omega_p) \rangle^{L_p} + \sum_{p' \neq p} \langle \Phi_{pp'}(\mathbf{u}_p, \omega_p, \mathbf{u}_{p'}, \omega_{p'}) \rangle^{L_p L_{p'} T_{p'}} , \quad (2a)$$

$$H_p^L(\omega_p) = L(\omega_p) + \langle V_p(\mathbf{u}_p, \omega_p) \rangle^{T_p} + \sum_{p' \neq p} \langle \Phi_{pp'}(\mathbf{u}_p, \omega_p, \mathbf{u}_{p'}, \omega_{p'}) \rangle^{L_{p'} T_p T_{p'}} , \quad (2b)$$

where $\langle X \rangle^{K_p}$ means the thermodynamic average of an operator X over the eigenstates of H_p^K with $K = T$ or L . From these equations it follows that the translational and rotational Hamiltonians are coupled and we have to solve the problem in an iterative way. The translational Hamiltonian is diagonalized in a basis of three-dimensional spherical harmonic-oscillator functions.²⁷ The basis for the rotational Hamiltonian consists of tesseral harmonics (real combinations of spherical harmonics).

The single-molecule eigenstates for the translations and rotations can then be used to calculate the collective excitations of the adsorbed layer. For this purpose we use the time-dependent Hartree method,^{27,28} which, at zero temperature, is equivalent to the random-phase approximation (RPA). In the TDH method the excitation energies are the eigenvalues of the matrix

$$\mathbf{M}(\mathbf{q}) = \begin{bmatrix} \chi - \mathbf{P}\Phi(\mathbf{q}) & -\mathbf{P}\Phi(\mathbf{q}) \\ \mathbf{P}\Phi(\mathbf{q}) & -\chi + \mathbf{P}\Phi(\mathbf{q}) \end{bmatrix} . \quad (3)$$

The diagonal matrixes χ and \mathbf{P} contain the mean-field excitation energies and the mean-field population differences

$$\chi_{abiK; a'b'i'K'} = \delta_{aa'} \delta_{bb'} \delta_{ii'} \delta_{KK'} (\epsilon_{iK}^{(a)} - \epsilon_{iK}^{(b)}) , \quad (4)$$

$$P_{abiK; a'b'i'K'} = \delta_{aa'} \delta_{bb'} \delta_{ii'} \delta_{KK'} (P_{iK}^{(a)} - P_{iK}^{(b)}) . \quad (5)$$

$\epsilon_{iK}^{(a)}$ is the mean-field energy of excitation level *a* of a molecule of sublattice *i* and $K = T$ or L . The population of this excitation level is given by

$$P_{iK}^{(a)} = \frac{\exp(-\beta \epsilon_{iK}^{(a)})}{\sum_b \exp(-\beta \epsilon_{iK}^{(b)})} \quad (6)$$

with $\beta = (kT)^{-1}$.

The matrix $\Phi(\mathbf{q})$ describes the coupling between the mean-field excitations on different molecules, as well as translation-rotation coupling

$$\begin{aligned} \Phi_{abiK;a'b'i'K'}(\mathbf{q}) = & \sum_{\mathbf{n}} \exp(i\mathbf{q} \cdot \mathbf{R}_{\mathbf{n}}) \langle \psi_{iK}^{(a)} \psi_{i'K'}^{(b')} | \langle \Phi_{\{0,i\}\{\mathbf{n},i'\}} \rangle^{iK_c; i'K'_c} | \psi_{iK}^{(b)} \psi_{i'K'}^{(a')} \rangle \\ & + \delta_{ii'} \delta_{KK'} \sum_{\mathbf{n}''} \sum_{i''} \langle \psi_{iK}^{(a)} \psi_{i'K'}^{(b')} | \langle \Phi_{\{0,i\}\{\mathbf{n}'',i''\}} \rangle^{i''K_c; i''K'_c} | \psi_{iK}^{(b)} \psi_{i'K'}^{(a')} \rangle + \delta_{ii'} \delta_{KK'} \langle \psi_{iK}^{(a)} \psi_{i'K'}^{(b')} | \mathcal{V}_{\{0,i\}} | \psi_{iK}^{(b)} \psi_{i'K'}^{(a')} \rangle, \end{aligned} \quad (7)$$

where $\psi_{iK}^{(a)}$ is the mean-field wave function corresponding with $\varepsilon_{iK}^{(a)}$, \mathbf{q} is the wave vector of the collective excitation, \mathbf{n} and \mathbf{n}'' label the unit cells, and K_c is the complement of K . The TDH matrix contains elements with $K \neq K'$. These elements mix the translations and rotations so that the translation-rotation coupling which was neglected in the mean-field treatment is restored by the TDH method.

B. The intermolecular potential

The intermolecular potential is written in the form of a spherical expansion

$$\Phi_{pp'}(\mathbf{u}_p, \boldsymbol{\omega}_p, \mathbf{u}_{p'}, \boldsymbol{\omega}_{p'}) = \sum_l \varphi_l(r_{pp'}) \sum_{\mathbf{m}} \begin{bmatrix} l_1 & l_2 & l_3 \\ m_1 & m_2 & m_3 \end{bmatrix} C_{m_1}^{(l_1)}(\boldsymbol{\omega}_p) C_{m_2}^{(l_2)}(\boldsymbol{\omega}_{p'}) C_{m_3}^{(l_3)}(\hat{\mathbf{r}}_{pp'}). \quad (8)$$

The intermolecular vector is given by

$$\mathbf{r}_{pp'} = (\mathbf{R}_{p'} + \mathbf{u}_{p'}) - (\mathbf{R}_p + \mathbf{u}_p)$$

and $\hat{\mathbf{r}}_{pp'}$ is the unit vector along $\mathbf{r}_{pp'}$. The Racah spherical harmonics $C_m^{(l)}(\boldsymbol{\omega})$ that describe the orientational dependence of the potential are coupled to a scalar function by the summation over $\mathbf{m} = \{m_1, m_2, m_3\}$, with the large parentheses denoting a 3- j symbol.²⁹ The first summation runs over $l = \{l_1, l_2, l_3\}$ and the factors $\varphi_l(r_{pp'})$ are the expansion of coefficients that reflect the anisotropy of the potential. They will be specified in Sec. III.

A Taylor expansion of the potential can be made in both the molecular displacements \mathbf{u}_p and $\mathbf{u}_{p'}$, so that the potential becomes explicitly dependent on these displacements. This expansion is amply described in Refs. 26 and 27 and the resulting form of the potential looks as follows:

$$\begin{aligned} \Phi_{pp'}(\mathbf{u}_p, \boldsymbol{\omega}_p, \mathbf{u}_{p'}, \boldsymbol{\omega}_{p'}) = & \sum_{\Lambda_1} \sum_{\Lambda_2} (u_p)^{\alpha_1} C_{\mu_1}^{(\lambda_1)}(\hat{\mathbf{u}}_p) \\ & \times C_{m_1}^{(l_1)}(\boldsymbol{\omega}_p) X_{\Lambda_1 \Lambda_2}(\mathbf{R}_{pp'}) \\ & \times (u_{p'})^{\alpha_2} C_{\mu_2}^{(\lambda_2)}(\hat{\mathbf{u}}_{p'}) \\ & \times C_{m_2}^{(l_2)}(\boldsymbol{\omega}_{p'}), \end{aligned} \quad (9)$$

where Λ stands for the set of indices $\{\alpha, \lambda, \mu, l, m\}$ and the expression for $X_{\Lambda_1 \Lambda_2}(\mathbf{R}_{pp'})$ is given in Ref. 26. The summations over α_1 and α_2 extends to $\alpha_1 + \alpha_2 \leq \alpha_{\max}$, where α_{\max} is equal to the order of the Taylor expansion in the displacements. An expansion with $\alpha_{\max} = 2$, for instance, yields a potential $\Phi_{pp'}$ which is harmonic in the center-of-mass displacements \mathbf{u}_p and $\mathbf{u}_{p'}$. In the present calculations we carry this expansion much further, see Sec. III. For the summations over λ and μ holds: $0 \leq \lambda_i \leq \alpha_i$ and $-\lambda_i \leq \mu_i < \lambda_i$, where λ_i has the same parity as α_i . After this expansion we have a potential which is explicitly dependent on the displacement coordinates of the molecules and thus easy to use in lattice-dynamics calculations.

C. The molecule-substrate potential

Following previous calculations,^{20,21} we consider the interaction V_p of a molecule p with the substrate as a sum of pair interactions between the molecule and the individual substrate atoms. The most general form for such molecule-atom interactions is, of course, a spherical expansion, i.e., a special case of Eq. (8). From selective adsorption measurements,²⁴ only the first, isotropic, term in such an expansion is known. As we wish to also investigate the effects of the anisotropy in the molecule-substrate interaction, we model this interaction by the atom-atom model, which contains this anisotropy implicitly. So we write,

$$\begin{aligned} V_p(\mathbf{u}_p, \boldsymbol{\omega}_p) = & \sum_C [v(|\mathbf{R}_p + \mathbf{u}_p + \mathbf{a}(\boldsymbol{\omega}_p) - \mathbf{R}_C|) \\ & + v(|\mathbf{R}_p + \mathbf{u}_p - \mathbf{a}(\boldsymbol{\omega}_p) - \mathbf{R}_C|)], \end{aligned} \quad (10)$$

where the vectors \mathbf{R}_C denote the positions of the carbon atoms C in the substrate and the orientation dependent vectors $\mathbf{a}(\boldsymbol{\omega}_p)$ describe the positions of the hydrogen atoms with respect to the H₂ center of mass. Just as Novaco and Wroblewski,²¹ we choose an atom-atom potential $v(|\mathbf{r}|)$ of the Lennard-Jones type, which is parametrized in such a manner that the isotropic component of the resulting molecule-atom potential agrees with the isotropic potential from the selective adsorption measurements (see Sec. III).

In Ref. 30 it is shown that the atom-atom interactions can be summed to an atom-substrate interaction with the aid of an analytical Fourier transformation. Next, a spherical expansion of the molecule-substrate interaction can be made to expose its anisotropy explicitly and, finally, a molecular-displacement expansion of the spherical expansion is used to make the molecule-substrate potential explicitly dependent on the displacement coordinates of the molecule.³¹ The molecule-substrate potential can then be written in the following form:

$$V_p(\mathbf{u}_p, \boldsymbol{\omega}_p) = \sum_{\Lambda} F_{\Lambda}(\mathbf{R}_p) (u_p)^{\alpha} C_{\mu}^{(\lambda)}(\hat{\mathbf{u}}_p) C_m^{(l)}(\boldsymbol{\omega}_p), \quad (11)$$

where, again, Λ indicates the set of indices $\{\alpha, \lambda, \mu, l, m\}$.

The coefficients $F_\Lambda(\mathbf{R}_p)$ can be written as a two-dimensional Fourier series

$$F_\Lambda(\mathbf{R}_p) = \sum_{\mathbf{g}} \bar{F}_\Lambda(\mathbf{g}|z_p) \exp(i\mathbf{g} \cdot \boldsymbol{\tau}_p) \quad (12)$$

with $\boldsymbol{\tau}_p$ denoting the projection of \mathbf{R}_p on the graphite basal plane (the xy plane), so that $\mathbf{R}_p = \boldsymbol{\tau}_p + z_p \mathbf{e}_z$. The vector \mathbf{g} is a vector in the two-dimensional reciprocal lattice of a substrate layer.

Analytical expressions for the expansion coefficients $\bar{F}_\Lambda(\mathbf{g}|z_p)$ are given in Ref. 31. The terms with $\mathbf{g}=\mathbf{0}$ describe the flat (but anisotropic and anharmonic) potential which depends only on the height z_p of the molecules above the graphite surface, the terms with $\mathbf{g} \neq \mathbf{0}$ contain the effects of the surface corrugation.

D. Analytical model for the roton bands

Due to the large rotational constants of H_2 and D_2 , the rotational excitation (roton) energies are rather large ($\approx 360 \text{ cm}^{-1}$ for $p\text{-H}_2$ and $\approx 180 \text{ cm}^{-1}$ for $o\text{-D}_2$). Since the typical excitation energies for the translational vibrations (phonons) are much lower (see Sec. IV), one expects

$$\tilde{X}_{l_1 m_1; l_2 m_2}(\mathbf{R}_{pp'}) = \sum_{\alpha_1 \lambda_1 \mu_1} \sum_{\alpha_2 \lambda_2 \mu_2} \langle (u_p)^{\alpha_1} C_{\mu_1}^{(\lambda_1)}(\hat{\mathbf{u}}_p) \rangle^{T_p} X_{\Lambda_1 \Lambda_2}(\mathbf{R}_{pp'}) \langle (u_{p'})^{\alpha_2} C_{\mu_2}^{(\lambda_2)}(\hat{\mathbf{u}}_{p'}) \rangle^{T_{p'}}. \quad (15)$$

For the systems under consideration, one can make several approximations. The only significant terms in the intermolecular potential and in the molecule-substrate potential are the terms with $l_1, l_2 \leq 2$ and $l \leq 2$ (see Sec. III). The terms that are relevant for the roton frequencies are the anisotropic interactions with l_1, l_2 , or $l \neq 0$. Because of the sixfold symmetry at the adsorption sites, the terms with $m \neq 0$ vanish. In the ground state of $p\text{-H}_2$ and $o\text{-D}_2$, the molecules are very nearly in a pure $j=0$ state. So, the expectation values $\langle C_m^{(l)}(\omega_p) \rangle^{L_p}$ are practically zero, except for $l=m=0$. Using all these simplifications, we are left with the following rotational mean-field Hamiltonian:

$$H^L(\omega_p) = BJ^2(\omega_p) + v_2 C_0^{(2)}(\omega_p), \quad (16)$$

where B is the rotational constant of H_2 or D_2 , J^2 is the molecular total angular-momentum operator, and v_2 is the strength of the anisotropic crystal field at the adsorption sites

$$v_2 = \bar{F}_{2,0}(\mathbf{R}_p) + \sum_{p' \neq p} \tilde{X}_{2,0;0,0}(\mathbf{R}_{pp'}). \quad (17)$$

The first contribution to this crystal field originates from the molecule-substrate interactions, the second term from the anisotropic interactions between the molecules in the adsorbed layer. Diagonalizing this Hamiltonian in a basis of spherical harmonics $Y_m^{(j)}(\omega_p)$ with $j=0$ and 2 , we find that only the states with $m=0$ are mixed

little mixing between the rotons and the phonons. The dependence of the roton band structure on the anisotropy of the intermolecular potential and of the molecule-substrate potential may be derived analytically. Since the latter anisotropy is not known, this will be very useful in the interpretation of (future) experimental data.

After substitution of Eq. (9) for the intermolecular potential and Eq. (11) for the molecule-substrate potential into Eq. (2b), we can write the rotational mean-field Hamiltonian as

$$H_p^L(\omega_p) = L(\omega_p) + \sum_{lm} \bar{F}_{lm}(\mathbf{R}_p) C_m^{(l)}(\omega_p) + \sum_{p' \neq p} \sum_{l_1 l_2} \sum_{m_1 m_2} \tilde{X}_{l_1 m_1; l_2 m_2}(\mathbf{R}_{pp'}) \times C_{m_1}^{(l_1)}(\omega_p) \langle C_{m_2}^{(l_2)}(\omega_{p'}) \rangle^{L_{p'}} \quad (13)$$

with

$$\bar{F}_{lm}(\mathbf{R}_p) = \sum_{\alpha \lambda \mu} F_\Lambda(\mathbf{R}_p) \langle (u_p)^\alpha C_\mu^{(\lambda)}(\hat{\mathbf{u}}_p) \rangle^{T_p} \quad (14)$$

and

$$\begin{aligned} \psi^{(0)} &= Y_0^{(0)} - \delta Y_0^{(2)}, \\ \psi^{(1)} &= Y_0^{(2)} + \delta Y_0^{(0)}, \end{aligned} \quad (18)$$

with the mixing coefficient δ given by

$$\delta \approx \frac{9\sqrt{5}}{245} \frac{v_2}{B}. \quad (19)$$

The corresponding mean-field energies are

$$\begin{aligned} \epsilon^{(0)} &\approx -\frac{9}{245} \frac{v_2^2}{B}, \\ \epsilon^{(1)} &\approx 6B + \frac{2}{7} v_2 + \frac{9}{245} \frac{v_2^2}{B}. \end{aligned} \quad (20)$$

The eigenstates $\psi^{(2)}$, $\psi^{(3)}$, $\psi^{(4)}$, and $\psi^{(5)}$ with $m \neq 0$ are the pure basis functions $Y_m^{(2)}$ with $m = \pm 1$ and ± 2 and the corresponding eigenvalues are

$$\begin{aligned} \epsilon^{(2,3)} &= 6B + \frac{1}{7} v_2, \\ \epsilon^{(4,5)} &= 6B - \frac{2}{7} v_2. \end{aligned} \quad (21)$$

The roton frequencies are the eigenvalues of the TDH matrix in Eq. (3), restricted to the pure rotational excitations $(0) \rightarrow (1), (2), (3), (4), (5)$. We take $T=0 \text{ K}$ so that the matrix \mathbf{P} becomes minus the unit matrix and we rewrite the eigenvalue problem for the matrix in Eq. (3) into the following eigenvalue equation:

$$\chi^{1/2}[\chi + 2\Phi(\mathbf{q})]\chi^{1/2}\mathbf{x}(\mathbf{q}) = \mathbf{x}(\mathbf{q})\Omega^2(\mathbf{q}) . \quad (22)$$

The diagonal matrix χ is now defined as

$$\Phi_{aa'}(\mathbf{q}) = 3Q^2\sqrt{70} \sum_{m_1 m_2 m_3} \begin{bmatrix} 2 & 2 & 4 \\ m_1 & m_2 & m_3 \end{bmatrix} \langle \psi^{(a)} | C_{m_1}^{(2)} | \psi^{(0)} \rangle \langle \psi^{(0)} | C_{m_2}^{(2)} | \psi^{(a')} \rangle \sum_n \exp(i\mathbf{q} \cdot \mathbf{R}_n) \langle r_{0n}^{-5} C_{m_3}^{(4)}(\hat{\mathbf{r}}_{0n}) \rangle^{T_0 T_n} . \quad (24)$$

Here, we have used the fact that all the adsorbed molecules are equivalent. Moreover, we have observed that the anisotropic intermolecular interactions with $l_1 = l_2 = 2$ are dominated by the quadrupole-quadrupole interactions (Q is the molecular quadrupole moment of H₂). The eigenvalue matrix $\Omega^2(\mathbf{q})$ obtained by solving Eq. (22) contains the squares of the roton frequencies $\omega_a(\mathbf{q})$ on the diagonal.

It follows from Eq. (24) that, for $\mathbf{q} = \mathbf{0}$, the matrix $\Phi(\mathbf{q})$ is diagonal. This is related to the sixfold symmetry of the adsorption sites which causes only the terms with $m_3 = 0$ to survive. This leads to $m_1 = -m_2$ and, since the mean-field states $\psi^{(a)}$ are characterized by quantum numbers m , we find immediately that $\Phi(0)$ is diagonal with elements

$$\begin{aligned} \Phi_{1,1}(0) &= \frac{6}{5}S , \\ \Phi_{2,2}(0) &= \Phi_{3,3}(0) = -\frac{4}{5}S , \\ \Phi_{4,4}(0) &= \Phi_{5,5}(0) = \frac{1}{5}S , \end{aligned} \quad (25)$$

where S is the two-dimensional quadrupole-quadrupole lattice sum

$$S = Q^2 \sum_n \langle r_{0n}^{-5} C_0^{(4)}(\hat{\mathbf{r}}_{0n}) \rangle^{T_0 T_n} . \quad (26)$$

For the optical roton frequencies we obtain, from Eq. (22),

$$\omega_a(0) = \{(\varepsilon^{(a)} - \varepsilon^{(0)})[\varepsilon^{(a)} - \varepsilon^{(0)} + 2\Phi_{aa}(0)]\}^{1/2} . \quad (27)$$

The crystal-field strength v_2 from Eq. (17) and the quadrupole-quadrupole coupling S are much smaller than the rotational energy splitting $6B$. In very good approximation we find that the roton frequencies are given by

$$\begin{aligned} \omega_1(0) &= 6B + \frac{6}{5}S + \frac{2}{7}v_2 + \frac{18}{245} \frac{v_2^2}{B} \quad \text{for } m = 0 , \\ \omega_{2,3}(0) &= 6B - \frac{4}{5}S + \frac{1}{7}v_2 + \frac{9}{245} \frac{v_2^2}{B} \quad \text{for } m = \pm 1 , \\ \omega_{4,5}(0) &= 6B + \frac{1}{5}S - \frac{2}{7}v_2 + \frac{9}{245} \frac{v_2^2}{B} \quad \text{for } m = \pm 2 . \end{aligned} \quad (28)$$

In this approximation the splittings between the roton frequencies for $\mathbf{q} = \mathbf{0}$ are additively determined by two contributions: the quadrupole-quadrupole lattice sum S and the effects caused by the crystal field v_2 . For general wave vectors, the quadrupole-quadrupole interaction matrix $\Phi(\mathbf{q})$ is no longer diagonal but, essentially, we obtain the same additivity. The crystal field leads to splittings

$$\chi_{aa'} = \delta_{aa'}(\varepsilon^{(a)} - \varepsilon^{(0)}) , \quad (23)$$

and the Fourier-transformed anisotropic coupling matrix can be written as

between the roton subbands of different $|m|$, the quadrupole-quadrupole coupling leads to dispersion of these subbands. Degeneracies between the different branches cause avoided crossings. Roton bands calculated for different v_2 will be discussed in Sec. IV. According to Eq. (28) we can directly obtain the strength of the anisotropic crystal field v_2 and, in particular, the unknown contribution $\bar{F}_{2,0}(\mathbf{R}_p)$ of the molecule-substrate interaction from the splittings between the subbands.

III. COMPUTATIONAL ASPECTS

The intermolecular potential used in our calculations is an *ab initio* calculated H₂-H₂ potential of Schäfer and Meyer²² improved by Schäfer and Köhler²³ through a multiproperty analysis. This potential is represented by a spherical expansion, Eq. (8), with all the anisotropic contributions for $l_1, l_2 \leq 2$. Each expansion coefficient $\varphi_l(r)$ consists of dispersion contributions ($\sim r^{-6}$, r^{-8} , and r^{-10}) and a short-range contribution which depends exponentially on r . The quadrupole-quadrupole interaction ($\sim r^{-5}$) appears in the $l_1, l_2, l_3 = 2, 2, 4$ term. This potential has been used in lattice-dynamics calculations on solid H₂ and D₂ (Ref. 26) and has proved to yield satisfactory results.

The modeling of the anisotropic molecule-substrate potential is described in Sec. II C. Our atom-atom model parameters are fitted to the empirical isotropic C-H₂ potential determined by selective adsorption measurements.²⁴ The Lennard-Jones parameters that were derived from these measurements are $\sigma_{\text{C-H}_2} = 2.89 \text{ \AA}$ and $\varepsilon_{\text{C-H}_2} = 0.3753 \text{ kJ/mol}$. We choose the Lennard-Jones parameters for the atom-atom C-H potential so that the isotropic term of the expansion in Eq. (11) (when restricted to only one carbon atom) matches the empirical isotropic C-H₂ potential. Thus, the anisotropic part of the molecule-substrate potential is determined by the separation of the two hydrogen atoms. If we use the experimental bond length of the hydrogen molecule (0.7417 Å), the Lennard-Jones parameters for the C-H interaction are $\sigma_{\text{C-H}} = 2.76 \text{ \AA}$ and $\varepsilon_{\text{C-H}} = 0.2184 \text{ kJ/mol}$. By changing the apparent bond length, we can scale the anisotropy, just as done in Ref. 21. With these parameters we find that the isotropic term of the molecule-substrate potential has a minimum above the centers of the carbon rings at $z = 2.785 \text{ \AA}$.

In previous lattice-dynamics calculations on bulk hydrogen, it was shown that, due to the large zero-point motions of the hydrogen molecules, the displacement ex-

pansion of the potential should not be truncated before the sixth-order terms.²⁶ Both for the intermolecular and for the molecule-substrate potential we have therefore extended the displacement expansion to $\alpha_{\max}=6$. The spherical expansion of the molecule-substrate potential is only extended to $l_{\max}=2$ because of the weak anisotropy of the hydrogen molecules.

The two-dimensional character of the adsorbed layer causes the translational motions of the molecules to be strongly anisotropic. The amplitude of the in-plane vibrations turns out to be very different from that of the out-of-plane vibration. Therefore, a large basis of spherical harmonic-oscillator functions is needed for the translational motions. With harmonic-oscillator functions up to $n_{\max}=8$, which results in a basis of 165 functions, the results are well converged. In these spherical harmonic-oscillator functions occurs a scaling parameter A which is used to optimized the basis.²⁷ For a three-dimensional isotropic oscillator $A=(M\omega/\hbar)^{1/2}$, where M is the molecular mass and ω the harmonic-oscillator frequency. In the case of an adsorbed layer, with the in-plane frequencies very different from the out-of-plane frequency, we average over the three fundamental excitations

$$A = \left[M \frac{[(\epsilon^{(1)} - \epsilon^{(0)}) + (\epsilon^{(2)} - \epsilon^{(0)}) + (\epsilon^{(3)} - \epsilon^{(0)})]}{3\hbar^2} \right]^{1/2}, \quad (29)$$

which yields better convergence with the same number of basis functions. Because of the weakly anisotropic interactions, a small basis of tesseral harmonics up to $j_{\max}=2$ is sufficient for the calculation of the rotational mean-field states.

In all calculations we use 1.42 Å as the nearest-neighbor distance between the carbon atoms within a graphite layer and 3.37 Å as the distance between the graphite layers. The nearest-neighbor spacing between the adsorbed molecules in the $(\sqrt{3} \times \sqrt{3})R30^\circ$ overlayer then equals 4.26 Å. The range of the two-dimensional lattice summation over the intermolecular potential is set at 8.0 Å. From Ref. 31 it is clear that, only for the interaction of an adsorbed molecule with the top layer of the graphite substrate, the corrugation has to be considered. This is achieved by summation over the molecule-atom pair potentials within a range of 30 Å. The rest of the graphite crystal is taken into account by including in Eqs. (11) and (12) the first Fourier term ($\mathbf{g}=\mathbf{0}$) of the interaction with the next ten layers. For the rotational constant of hydrogen we take $B=59.06 \text{ cm}^{-1}$ and for deuterium $B=29.83 \text{ cm}^{-1}$. All calculations are performed at zero temperature.

IV. RESULTS AND DISCUSSION

From the single-particle states of the molecules calculated at the mean-field level, one can derive various quantities, such as the total Helmholtz free energy, the translational and rotational energy, and the expectation values of the displacements of the molecules. These are listed in Table I. Our first observation is that the vibrationally averaged height $\langle z \rangle$ of the molecules above the

graphite surface is substantially greater than the height $z_0=2.785 \text{ Å}$ of the equilibrium positions of the molecules. These equilibrium positions are calculated from the isotropic term in the molecule-substrate potential and they lie above the centers of the sixfold carbon rings. For $p\text{-H}_2$ and $o\text{-D}_2$ we find that $\langle u_z \rangle = \langle z \rangle - z_0$ equals 0.178 and 0.122 Å, respectively. This reflects the strong anharmonicity of the out-of-plane vibrations. Although the choice of origin should be irrelevant for a complete basis, we have located the basis functions for the translational vibrations at height $\langle z \rangle$ since this appears to yield the best converged results for a fixed number of basis functions.

We observe further a strong anisotropy in the translational vibrations. The root-mean-square amplitude of the in-plane vibrations is almost twice as large as the amplitude of the out-of-plane vibrations, both for $p\text{-H}_2$ and for $o\text{-D}_2$. We find good agreement with the amplitude of the in-plane vibrations in $o\text{-D}_2$ which has been determined from neutron-diffraction intensities.⁹

The TDH calculations yield the phonon and roton band structure, as well as possible mixing between these bands. Since the roton frequencies in $p\text{-H}_2$ and $o\text{-D}_2$ are considerably higher than the phonon frequencies, there is very little mixing, however, and we discuss the phonons and the rotons separately. In the calculations of the phonon bands we have included five excited center-of-mass vibrations of each molecule: the two fundamental in-plane vibrations, the fundamental out-of-plane vibration, and the two lowest in-plane overtones. The latter were taken into account because they appear to be nearly degenerate with the fundamental out-of-plane mode. Thus, one might expect Fermi resonances between these modes which will affect the phonon band structure, except in those points of the two-dimensional Brillouin zone where such resonances are forbidden by symmetry (e.g., the Γ point). The following characteristics of the in-plane phonon band structure have been determined by INS:¹⁰⁻¹⁵ the lowest phonon frequency at the Γ point (ω_0), the total width of the in-plane phonon band ($\Delta\omega$), the frequency of the transverse phonon at the M point (ω_T), and the frequency of the longitudinal phonon near the K point (ω_L). The mode with frequency ω_0 is an acoustical phonon mode (an overall translation of the entire adsorbed layer). The value of ω_0 (often called the phonon gap) is a direct measure for the corrugation in the substrate-adsorbed layer potential. The results which we have obtained for these quantities are shown in Table II, together with the experimental data and the results available from calculations by Novaco *et al.*^{20,21} and by Gottlieb *et al.*^{18,19} Phonon dispersion curves are displayed in Figs. 1 and 2.

The results from our TDH calculations lie very close to the in-plane phonon frequencies from the SCP calculations by Novaco.²⁰ Apparently these phonon frequencies are determined mainly by the isotropic potential. The isotropic term in the molecule-substrate potential is derived from selective adsorption measurements,²⁴ both in our calculations and in those of Novaco.²⁰ For the $\text{H}_2\text{-H}_2$ interactions he applies a semiempirical isotropic potential of Silvera and Goldman,³² whereas we use an anisotropic *ab initio* potential.^{22,23} Moreover, we include the out-of-

TABLE I. Helmholtz free energy (F), translational kinetic energy (E_T), and average displacements (at $T=0$ K) for commensurate p -H₂ and o -D₂ layers on graphite.

	This work	Ref. 20	Ref. 21	Ref. 19	Experimental 9
p -H ₂					
F (kJ/mol)	-3.963	-4.247			
E_T (kJ/mol)	0.776				
$\langle z \rangle$ (Å)	2.963	3.0	2.92		
$\langle u_z^2 \rangle - \langle u_z \rangle^2$ (Å ²)	0.053	0.04	0.042		
$\langle u_x^2 + u_y^2 \rangle$ (Å ²)	0.345		0.353	0.436	
o -D ₂					
F (kJ/mol)	-4.438	-4.717			
E_T (kJ/mol)	0.531				
$\langle z \rangle$ (Å)	2.907	2.9	2.88		
$\langle u_z^2 \rangle - \langle u_z \rangle^2$ (Å ²)	0.037	0.04	0.029		
$\langle u_x^2 + u_y^2 \rangle$ (Å ²)	0.270		0.268	0.328	0.25

plane phonons and the rotons, which we find to be well separated from the in-plane phonons, however. Our results are in good agreement with the experimental data;¹¹ the dispersion of the in-plane phonons is just slightly overestimated. We have also modeled the H₂-graphite interactions with empirical atom-atom potentials derived from solid hydrocarbons,³³ but the results appeared to be substantially worse.

From Figs. 1 and 2 it is obvious that the out-of-plane phonons mix with in-plane two-phonon states. The frequencies of the out-of-plane phonons are close to the out-of-plane vibrational frequency (122.4 cm⁻¹) of a single H₂ molecule obtained from selective adsorption measurements.²⁴ The frequency for the out-of-plane mode

which was deduced from the INS spectrum of p -H₂ on graphite¹⁵ is substantially higher, however (157 cm⁻¹). An alternative assignment of the INS spectrum¹⁵ might be suggested. This spectrum contains a strong peak at 118 cm⁻¹ which is due to the $j=0 \rightarrow 1$ rotational transition. This transition is optically forbidden, but it is induced by neutron scattering. We think that the out-of-plane phonons (calculated at 115.3 cm⁻¹ for $\mathbf{q}=0$) might be hidden under this peak. (Actually a side peak is observed at 114 cm⁻¹.) The broad peak around 157 cm⁻¹ should then be assigned, probably, to a combination band of the $j=0 \rightarrow 1$ rotational transitions or the out-of-plane phonons with the in-plane phonon modes. Such a com-

TABLE II. Phonon frequencies (in cm⁻¹). $\omega_0(E_1)$ is the phonon gap, i.e., the frequency of the E_1 mode at the Γ point (space group $p6mm$). $\Delta\omega$ is the bandwidth of the in-plane phonon band. ω_T is the frequency of the transversal phonon mode at the M point. ω_L is the frequency of the longitudinal phonon mode near the K point. $\omega(E_2)$ is the frequency of the in-plane two-phonon excitation at the Γ point. $\omega(A_1)$ is the frequency of the out-of-plane mode at the Γ point.

	This work	Ref. 20	Ref. 19	Experimental 11 and 15
p -H ₂				
$\omega_0(E_1)$	34.1	32.4	27.2	32.9
$\Delta\omega$	25.5	29.3		19.1
ω_T	45.7	45.1		40.2
ω_L	56.0	58.2		49.6
$\omega(E_2)$	107.6			
$\omega(A_1)$	115.3			(157)
o -D ₂				
$\omega_0(E_1)$	25.3	25.6	21.7	27.8
$\Delta\omega$	10.5	10.3		6.6
ω_T	30.8	30.7		30.8
ω_L	34.4	35.0		33.4
$\omega(E_2)$	67.7			
$\omega(A_1)$	71.3			

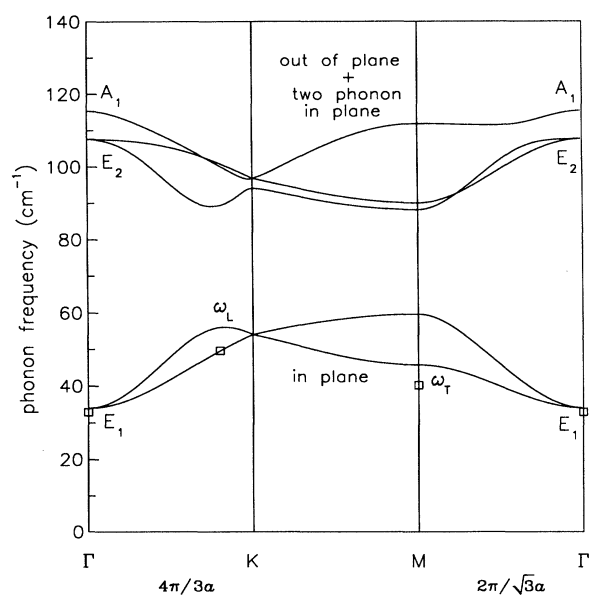


FIG. 1. Phonon dispersion curves for a p -H₂ monolayer on graphite, from TDH calculations at $T=0$ K, compared with the experimental values of ω_0 , ω_L , and ω_T (\square) from Refs. 11 and 12 ($a=4.26$ Å is the nearest-neighbor distance in the adsorbed layer).

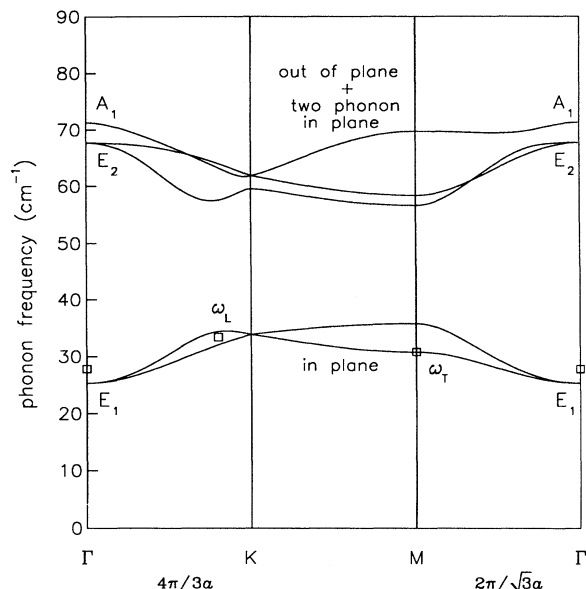


FIG. 2. Phonon dispersion curves for an *o*-D₂ monolayer on graphite, compared with the experimental values of ω_0 , ω_L , and ω_T (□) from Refs. 11 and 12.

bination band may range from 151 to 170 cm⁻¹ (4.53–5.08 THz) which is consistent with the broad peak in the experimental spectrum. If this alternative assignment is not correct, then we would have to conclude that the shift in the out-of-plane vibrational frequency from 122 cm⁻¹ for a single H₂ molecule to 157 cm⁻¹ for a full H₂ monolayer is caused by substrate-mediated interactions between the molecules in the adsorbed layer. In our

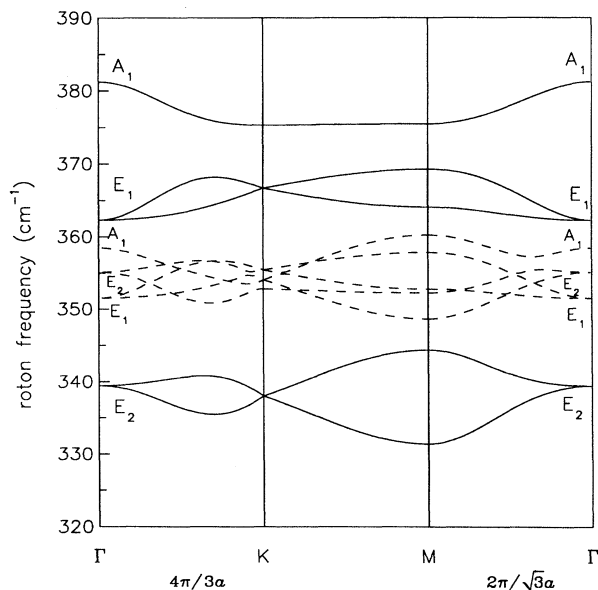


FIG. 3. Roton dispersion curves for a *p*-H₂ monolayer on graphite, from TDH calculations at $T=0$ K. Solid curves: with v_2 from Eq. (17). Dashed curves: with $v_2=0$.

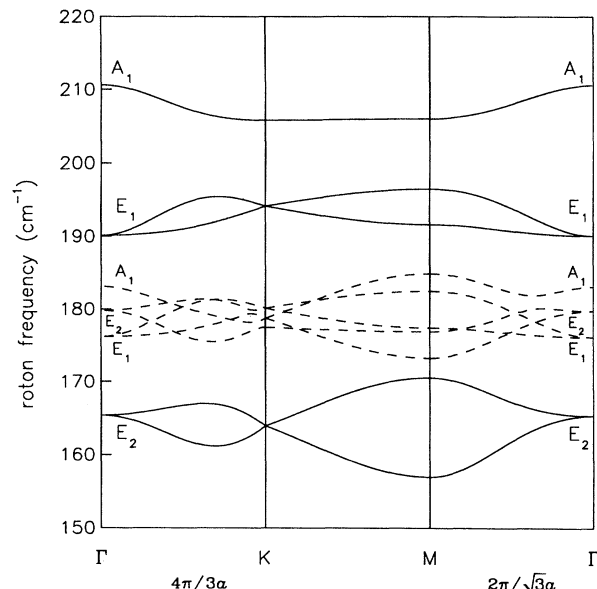


FIG. 4. Roton dispersion curves for an *o*-D₂ monolayer on graphite. Solid curves: with v_2 from Eq. (17). Dashed curves: with $v_2=0$.

calculations these interactions have been ignored. It would be surprising, however, if they affect so strongly the out-of-plane vibrations, while the in-plane modes are in good agreement with experiment. Therefore, we prefer the first explanation.

The structure of the roton bands for *p*-H₂ and *o*-D₂ layers on graphite is shown in Figs. 3 and 4. Since the anisotropy of the molecule-substrate potential is entirely unknown (see Secs. II C and II D), we have varied the strength of this anisotropy by changing the anisotropy parameter v_2 in the crystal field, see Eqs. (16) and (17). The dashed curves are obtained for $v_2=0$, the solid curves are calculated with the values of v_2 (65.1 cm⁻¹ for *p*-H₂ and 69.9 cm⁻¹ for *o*-D₂) that are obtained from the anisotropic H₂-H₂ potential within the layer, in combination with the atom-atom model for the H₂-substrate interaction (see Sec. II C). The latter values of v_2 are almost certainly overestimated as it is known that the atom-atom model overrates the asphericity of the H₂ molecule and it appears from NMR measurements¹⁷ for *o*-H₂ and *p*-D₂ on graphite that v_2 is probably rather small. It is obvious that the value of v_2 , which is dom-

TABLE III. Optical ($\mathbf{q}=0$) roton frequencies (in cm⁻¹), obtained from the full TDH calculations including phonons, and obtained from Eq. (28) with v_2 calculated from Eq. (17) and S from Eq. (26), see text.

<i>p6mm</i> symmetry	<i>p</i> -H ₂		<i>o</i> -D ₂	
	Eq. (28)	TDH	Eq. (28)	TDH
<i>E</i> ₂	339.0	339.5	165.7	165.4
<i>E</i> ₁	363.7	362.3	192.5	190.1
<i>A</i> ₁	382.1	381.2	214.9	210.6

inated by the anisotropy $\tilde{F}_{2,0}$ in the molecule-substrate interaction, see Eq. (17), has an enormous effect on the roton dispersion curves. This effect can be completely understood from the derivation in Sec. IID which leads to Eq. (28). One observes nearly parallel shifts of the roton subbands when v_2 is changed. The shape of these subbands, which is primarily determined by the quadrupole-quadrupole interactions within the adsorbed layer, is practically not altered, except for avoided crossings. From Table III it appears that the simple formula given by Eq. (28) is indeed capable of yielding rather accurate roton frequencies. This will be very valuable when these frequencies will be measured, because Eq. (28) allows the direct calculation of v_2 from the splittings between the (optical) roton frequencies. Experimental data for p -H₂ on graphite are available³⁴ from electron-energy-loss spectroscopy (EELS). A peak has been ob-

served at $379 \pm 16 \text{ cm}^{-1}$, which agrees, in particular, with the frequency of the calculated optical roton with polarization perpendicular to the surface (symmetry A_1). The resolution of these measurements was too low to observe any splittings. Moreover, the selection rules effective in EELS might prevent the observation of rotons polarized parallel to the surface.

ACKNOWLEDGMENTS

We thank Dr. V.L.P. Frank, Dr. H. J. Lauter, and Dr. H. Wiechert for communicating their results prior to publication. The investigations were supported in part by the Netherlands Foundation for Chemical Research (SON) with financial aid from the Netherlands Organization for Scientific Research (NWO).

-
- ¹J. Cui and S. C. Fain, Jr., *Phys. Rev. B* **39**, 8628 (1989).
²J. Cui, S. C. Fain, Jr., H. Freimuth, H. Weichert, H. P. Schildberg, and H. J. Lauter, *Phys. Rev. Lett.* **60**, 1848 (1988).
³H. P. Schildberg, H. J. Lauter, H. Freimuth, H. Wiechert, and R. Haensel, *Jpn. J. Appl. Phys.* **26**, 345 (1987).
⁴H. Freimuth, H. Wiechert, and H. J. Lauter, *Surf. Sci.* **189-190**, 548 (1987).
⁵H. J. Lauter, H. P. Schildberg, H. Godfrin, H. Wiechert, and R. Haensel, *Can. J. Phys.* **65**, 1435 (1987).
⁶M. Nielsen, J. P. McTague, and L. Passell, in *Phase Transitions in Surface Films*, edited by J. G. Dash and J. Ruvalds (Plenum, New York, 1980), p. 127.
⁷H. Freimuth and H. Wiechert, *Surf. Sci.* **178**, 716 (1986).
⁸H. Freimuth and H. Wiechert, *Surf. Sci.* **162**, 432 (1985).
⁹H. Freimuth, H. Wiechert, H. P. Schildberg, and H. J. Lauter (unpublished), cited in Refs. 12, and 19.
¹⁰M. Nielsen, J. P. McTague, and W. Ellenson, *J. Phys. (Paris) Colloq.* **38**, C4-10 (1977).
¹¹H. J. Lauter, V. L. P. Frank, P. Leiderer, and H. Wiechert, *Physica B* **156-157**, 280 (1989).
¹²V. L. P. Frank, H. J. Lauter, and P. Leiderer, *Phys. Rev. Lett.* **61**, 436 (1988).
¹³H. J. Lauter, in *Phonons 89*, edited by S. Hunklinger *et al.* (World-Scientific, Singapore, 1990), p. 871.
¹⁴V. L. P. Frank, H. J. Lauter, and P. Leiderer, in *Phonons 89*, edited by S. Hunklinger *et al.* (World-Scientific, Singapore, 1990), p. 913.
¹⁵J. L. Armony, V. L. P. Frank, H. J. Lauter, and P. Leiderer, in *Phonons 89*, edited by S. Hunklinger *et al.* (World-Scientific, Singapore, 1990), p. 916.
¹⁶A. B. Harris and A. J. Berlinski, *Can. J. Phys.* **57**, 1852 (1979).
¹⁷P. R. Kubik, W. N. Hardy, and H. Glattli, *Can. J. Phys.* **63**, 605 (1985).
¹⁸J. M. Gottlieb and L. W. Bruch, *Phys. Rev. B* **40**, 148 (1989).
¹⁹J. M. Gottlieb and L. W. Bruch, *Phys. Rev. B* **41**, 7195 (1990).
²⁰A. D. Novaco, *Phys. Rev. Lett.* **60**, 2058 (1988).
²¹A. D. Novaco and J. P. Wroblewski, *Phys. Rev. B* **39**, 11 364 (1989).
²²J. Schäfer and W. Meyer, *J. Chem. Phys.* **70**, 344 (1979).
²³J. Schäfer and W. Köhler, *Z. Phys. D* **13**, 217 (1989).
²⁴L. Mattera, F. Rosatelli, C. Salvo, F. Tommasini, U. Valbusa, and G. Vidali, *Surf. Sci.* **93**, 515 (1980).
²⁵M. Karimi and G. Vadali, *Surf. Sci.* **208**, L73 (1989).
²⁶W. B. J. M. Janssen and A. van der Avoird, *Phys. Rev. B* **42**, 838 (1990).
²⁷W. J. Briels, A. P. J. Jansen, and A. van der Avoird, *J. Chem. Phys.* **81**, 4118 (1984).
²⁸D. R. Fredkin and N. R. Werthamer, *Phys. Rev.* **138**, A1527 (1965).
²⁹D. M. Brink and G. R. Satchler, *Angular Momentum* (Clarendon, Oxford, 1975).
³⁰W. A. Steele, *Surf. Sci.* **36**, 317 (1973).
³¹T. H. M. van den Berg and A. van der Avoird, *Phys. Rev. B* **40**, 1932 (1989).
³²I. F. Silvera and V. V. Goldman, *J. Chem. Phys.* **69**, 4209 (1978).
³³D. E. Williams and T. L. Starr, *Comput. Chem.* **1**, 173 (1977).
³⁴R. E. Palmer and R. F. Willis, *Surf. Sci.* **179**, L1 (1987).